THE ASTROPHYSICAL JOURNAL, 516:335–341, 1999 May 1

GG TAURI'S CIRCUMBINARY DISK: MODELS FOR NEAR-INFRARED SCATTERED-LIGHT IMAGES AND ^{13}CO ($J = 1 \rightarrow 0$) LINE PROFILES

KENNETH WOOD,[1] MERCE CROSAS,[1] AND ANDREA GHEZ[2]
Received 1998 August 31; accepted 1998 December 8

ABSTRACT

We describe models that reproduce the observed near-IR scattered-light images and ^{13}CO ($J = 1 \rightarrow 0$) line profiles from the GG Tau circumbinary disk. The observed extent of the scattered-light images requires a 0.13 $M_\odot$ flared circumbinary disk (as determined from millimeter observations), an inner cleared region of 200 AU, and scale height of 16.6 AU at the disk's inner edge. To reproduce the brightness distribution, we require extinction of the illuminating starlight prior to scattering within the circumbinary disk. This extinction is obtained by including the effects of small circumstellar disks that are coplanar with the circumbinary disk. Further, we find that the effects of geometry and illumination allows the observed scattered-light pattern to be reproduced with a dust grain distribution that fits data from other Taurus-Auriga circumstellar environments. This indicates that unless geometries and illuminations are known, great care must be taken when attempting to determine grain properties from analysis of scattered-light images. The observed ^{13}CO line profiles are reproduced using the same geometry adopted for the near-IR modeling. However, we find that the ^{13}CO abundance is lower than in the diffuse interstellar medium, in agreement with previous investigations indicating CO depletion in circumstellar environments.

Subject headings: binaries: visual — circumstellar matter — radiative transfer — stars: individual (GG Tauri) — stars: pre–main-sequence

1. INTRODUCTION

Dense, equatorial circumstellar disks are predicted to form during the formation of single low-mass stars (Shu, Adams, & Lizano 1987). Their existence was originally observationally inferred from their signature of excess IR radiation arising from the reprocessing of starlight by dust and the liberation of accretion luminosity (Adams & Shu 1986; Adams, Lada, & Shu 1987; Kenyon & Hartmann 1987). Radio and millimeter investigations have also revealed disks and allowed their velocity and density structures to be probed (Koerner, Sargent, & Beckwith 1993a; Koerner & Sargent 1995; Beckwith & Sargent 1993; Beckwith et al. 1990). Recently, high-resolution optical images of circumstellar disks (Burrows et al. 1996; Stapelfeldt et al. 1998) have discovered disk structures predicted by radiation transfer models of disks viewed at arbitrary inclinations (Whitney & Hartmann 1992; Fischer, Henning, & Yorke 1994). While much effort has been devoted to theoretical modeling of the density structure and observational signatures of disks around single stars, it is only relatively recently, motivated by survey projects that have found companions to many stars, that attention has been focussed on the environments harboring multiple star systems. The three main binary star formation mechanisms are disk instabilities, capture, and core fragmentation (e.g., Pringle 1991; Clarke 1995). Recent observational evidence presented by Ghez, White, & Simon (1997) that the T Tauri systems they surveyed (including GG Tau) appeared to have stars that were coeval led them to favor core fragmentation for the formation of these systems.

Theoretical investigations have shown that binary motion within a circumbinary disk will lead to tidal truncation and clearing of the inner disk regions (Lin & Papaloizou 1993; Artymowicz & Lubow 1994, 1996). The first low-mass pre–main-sequence binary system in which definite detections of circumbinary material were found, appearing to match the dynamical predictions, was the GG Tau system. This quadruple system (comprising two close binaries) was found to possess a large rotating dusty ring around the northern (brighter and more massive) binary system (Simon & Guilloteau 1992; Dutrey, Guilloteau, & Simon 1994; Koerner, Sargent, & Beckwith 1993b). Analysis of their 2.6 mm continuum data and spatially resolved ^{13}CO ($J = 1 \rightarrow 0$) line profiles led Dutrey et al. to the conclusion that the northern binary in the GG Tau system was surrounded by a 0.13 $M_\odot$ Keplerian rotating disk (of dust plus gas) inclined at around 40° to the line of sight, with an outer radius of at least 800 AU, and an inner radius of 180 AU. Assuming that this disk was hydrostatically supported and the temperature and rotational velocity followed simple power laws with radius, Dutrey et al. estimated the disk scale height to be around 14 AU at a radius of 100 AU. They also found that models of the ^{13}CO line profiles (in the thin disk approximation) agreed well with their data, assuming that the disk is in Keplerian rotation and has around 90% of its mass in a dense ring of radius 180 AU.

The circumbinary disk has since been detected in the near-IR by Roddier et al. (1996) using the University of Hawaii's adaptive optics system. This data has kindly been provided to us by C. Roddier and is presented for comparison with our models in Figure 4. Roddier et al. found that most of the light scattered by the circumbinary disk was contained within two concentric ellipses with the same axial ratio ($b/a = 0.82$) and semimajor axes of 1.″25 and 1.″90, corresponding to physical sizes of 175 AU and 266 AU, respectively (assuming GG Tau is at a distance of 140 pc). On analyzing the scattered light, they found that it was redder than that of the central stars. Roddier et al. attrib-

[1] Smithsonian Astrophysical Observatory, 60 Garden Street, Cambridge, MA 02138;
kenny@claymore.harvard.edu, mcrosas@cfa.harvard.edu.
[2] Department of Physics & Astronomy, UCLA, Los Angeles, CA 90095; ghez@astro.ucla.edu, kenny@claymore.harvard.edu.

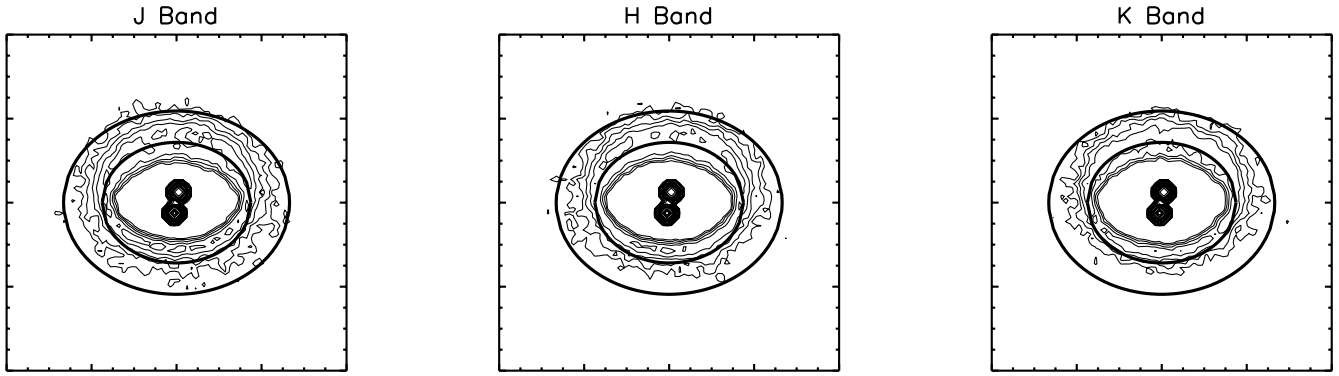

FIG. 1.—Scattered-light simulations for model 1 at J, H, and K viewed at an inclination of $i = 35°$. Each figure is 800 AU on a side. Also shown are the concentric ellipses that Roddier et al. (1996) found contained most of the scattered flux they observed. The lowest contour in each image is at 5×10^{-5} times the peak flux in each image and the contour spacing is at half-magnitude intervals.

uted this to extinction of the stellar radiation in circum*stellar* disks prior to scattering in the circum*binary* disk. Further evidence for small circumstellar disks is to be found in the spectra of the individual stars in the binary system—both stars exhibit a near-IR excess. On the whole, the agreement between the system parameters derived from the IR and millimeter images is very good with the deprojected binary separation being around 50 AU, inner disk radius of 200 AU, and an inclination angle between 35° (Roddier et al.) and 43° (Dutrey et al.).

Since no detailed modeling of the scattered-light images was attempted by Roddier et al. and only single scattering in a flat disk was considered by Close et al. (1998), in this paper we attempt to find a consistent model for the GG Tau circumbinary disk that fits both the IR scattered-light images and the ^{13}CO ($J = 1 \rightarrow 0$) data. We construct near-IR scattered-light images using a multiple scattering Monte Carlo radiation transfer code and match the model images to the size, shape, and brightness distribution of the data presented by Roddier et al. We also present detailed calculations of the ^{13}CO ($J = 1 \rightarrow 0$) transitions within the circumbinary disk using the Monte Carlo code developed by Crosas & Menten (1997). The CO calculations are performed using the same density structure that we use for our scattered-light models.

The layout of the paper is as follows: § 2 presents the circumbinary density structure and a summary of the Monte Carlo techniques used for the continuum and line radiation transfer, § 3 presents the results of our near IR modeling, § 4 presents the line profile calculations, and we conclude in § 5 with a summary of our findings and comparison to previous models for GG Tau.

2. MODEL PARAMETERS AND RADIATION TRANSFER TECHNIQUES

The density structure that we adopt for the circumbinary disk and the radiation transfer techniques utilized in the simulations have been described in other papers (e.g., Whitney & Hartmann 1992; Crosas & Menten 1997). We now give a brief summary of the ingredients of our simulations.

The circumbinary disk density is that of a standard flared disk

$$\rho = \rho_0 \exp[-(z/h)^2/2]/r^{\alpha}\,, \qquad (1)$$

with a scale height that increases with radius as $h = h_0(r/R_0)^{\beta}$ (Shakura & Sunyaev 1974). We set $R_0 = 100$ AU. For our scattered-light models we set the mass of the circumbinary disk to be 0.13 $M_{\odot}$ (Simon & Guilloteau 1992) and the outer disk radius at 800 AU. Throughout we assume a radial density exponent $\alpha = 2$. Dutrey et al. (1994) modeled the circumbinary disk with $h_0 = 14.5$ AU, inner disk radius of 180 AU, and $\beta = \frac{5}{4}$ (this value of β arises from the assumption that the disk temperature $T \propto r^{-1/2}$). In our simulations, we keep $\beta = \frac{5}{4}$ as proposed by Dutrey et al. In principle we could have varied β within the generally accepted range of $\frac{9}{8} \leq \beta \leq \frac{5}{4}$, which arises from radial temperature profiles $T(r) \propto r^{-3/4}$ and $r^{-1/2}$ (e.g., Kenyon & Hartmann 1987). However, there exist degeneracies between h_0, β, and α such that so long as the scale height at large radii is fixed, the scattered-light images appear very similar (e.g., Wood et al. 1998; Burrows et al. 1996).

We construct model scattered-light images with a Monte Carlo continuum radiation transfer code that accounts for multiple photon scattering and predicts the spatially resolved flux and polarization (Whitney & Hartmann 1992; Whitney, Kenyon, & Gomez 1997; Wood et al. 1998). The model images are convolved with a Gaussian point spread function of FWHM = 15 AU, which is comparable to the 0.″1 resolution of the adaptive optics images obtained by Roddier et al. (1996). We assume that all radiation originates from two point sources separated by 50 AU. The number of photons released from each star in the binary system is determined by the luminosity ratios at $J = 2.25{:}1$, $H = 2.09{:}1$, and $K = 2.09{:}1$, given by Roddier et al. (their Table 4). In the radiation transfer calculation, the dust and gas mixture has a total opacity, κ, albedo, a, and a scattering phase function approximated by the Henyey-Greenstein phase function (Henyey & Greenstein 1941) with asymmetry parameter, g. We choose to model the disk opacity using a Kim, Martin, & Hendry (1994) grain mixture. The adopted parameters (κ, a, and g) presented in Table 1 are for the total gas plus dust mixture. Whitney et al. (1997) showed that the Kim et al. (1994) grain mixture successfully reproduces the colors of class I sources in Taurus, but it tends to underestimate the polarization of the Taurus protostars. We keep the dust parameters fixed throughout our simulations.

The line transfer is performed using the Monte Carlo technique described by Crosas & Menten (1997) and is based on that developed by Bernes (1979). The initial spher-

TABLE 1

DUST PARAMETERS

Band	κ (cm^2 g^{-1})	a	g
J ...	63	0.46	0.32
H ...	38	0.42	0.29
K ...	22	0.35	0.25

ically symmetric model has been modified to an axisymmetric model for this case. The flared disk is contained in a cylinder, which is divided into 60 × 60 rings of the same height and width. Statistical balance is applied at every ring, and the level populations are calculated by using the same Monte Carlo technique used in the spherically symmetric case. The photons emitted by ^{13}CO molecules in the disk and external cosmic microwave background photons are followed throughout the disk until they escape or are absorbed. We consider 12 rotational levels for ^{13}CO and include spontaneous emissions, stimulated absorptions and emissions, and collisional excitations and deexcitations. Density and temperature are varied at every ring, and the ^{13}CO abundance is constant within the disk. We assume that the disk is in Keplerian rotation. The line emission is calculated by integrating along the line of sight for 60 × 60 impact parameters (which, because of the disk inclination, do not correspond to the rings of the geometrical disk), and applying the Euler angles to take into account the inclination of the disk with respect to the observer.

3. OPTICAL AND NEAR-IR SCATTERED-LIGHT IMAGES

In the following sections we present our near-IR scattered-light models for the GG Tau system. Table 2 shows the parameters we varied for the scattered-light simulations. The features observed by Roddier et al. (1996) that we wish to reproduce are: (1) the physical extent of the circumbinary disk defined by concentric ellipses with axial ratio $b/a = 0.82$ and semimajor axes of 1.″25 and 1.″90; (2) the ratio of scattered to direct light, R_λ; and (3) the ratio of light scattered off the near and far sides of the disk, NF_λ. We define a successful scattered-light model as one that matches these three criteria. The flux ratios R_λ and NF_λ are defined as follows. The ratio R_λ is the total flux contained within the concentric ellipses, divided by the flux within the central ellipse. This is essentially the ratio of scattered to direct flux. The second ratio, NF_λ, is the ratio of scattered flux lying within the lower half of the concentric ellipses to that in the upper half. This ratio is to be compared with the near/far ratios modeled by Close et al. (1998). When modeling the near/far ratios, Close et al. calculated the ratio of single scattered flux from two diametrically opposite points on a flat circumbinary disk. Whereas the model of Close et al. measures the asymmetry in the dust scattering phase function for light scattered through $\pi/2 - i$ and $\pi/2 + i$, (i is the inclination of the circumbinary disk), our NF_λ ratios measure the asymmetry of the scattered light from the front and rear parts of the disk as a whole including the effects of illumination, multiple scattering, and a nonplanar circumbinary disk. The scattered-light ratios measured by Roddier et al. and results of our simulations are presented in Table 3, on the model images we overplot the concentric ellipses. We first show the simulations when the circumbinary disk is illuminated by two isotropic point sources.

3.1. *Naked Binary Stars*

Figure 1 shows near-IR simulations for model 1 that uses the density structure of equation 1 with disk parameters from Dutrey et al. (see Table 2) and luminosity ratio from Roddier et al. (their Table 4). We ran simulations with different values for the system inclination and found that $i = 35°$ gives the best fit to the data—the scattered-light patterns for lower or higher inclinations did not lie within the concentric ellipses defined by Roddier et al. (1996). The dynamic range of these images is very large, with the flux levels from the circumbinary disk being around $10^{-4}\ F_\star$. On these contour images we have overlaid the concentric ellipses defined by Roddier et al., which they found contained the majority of the scattered flux. In our model, since we have truncated the disk at an inner radius, there is in effect a wall at the disk's inner edge. As a result, the scattered light from the far side of the disk is from light scattering off the inner edge of the disk, while on the near side we see light scattering off the surface of the inclined circumbinary disk. Clearly the Dutrey et al. (1994) density structure produces images that are too extended within the innermost ellipse defined by Roddier et al. We have also calculated flux ratios (Table 3) to compare with those measured by Roddier et al. We find that using the scale height proposed by Dutrey et al., the R_λ ratios are too large by a factor of 4–7. Also, Roddier et al. found that the near side of the disk is brighter than the far side—our NF_λ ratios for

TABLE 2

MODELS

Model	Circumstellar Disks	h_0 (AU)	R_{min} (AU)	R_{max} (AU)	M_{disk} ($M_\odot$)	β	α
1	No	14.5	180	800	0.13	1.25	2.0
2	No	7.0	200	800	0.13	1.25	2.0
3.....	$10^{-4}\ M_\odot$	7.0	200	800	0.13	1.25	2.0

TABLE 3

FLUX RATIOS

Parameter	R_J	R_H	R_K	NF_J	NF_H	NF_K
Observed.....	$(0.43 \pm 0.12) \times 10^{-2}$	$(0.78 \pm 0.08) \times 10^{-2}$	$(0.57 \pm 0.25) \times 10^{-2}$	3.6 ± 1.0	2.6 ± 0.25	1.5 ± 0.5
Model 1.....	3.00×10^{-2}	2.80×10^{-2}	2.30×10^{-2}	0.67	0.67	0.67
Model 2.....	3.0×10^{-2}	2.7×10^{-2}	2.2×10^{-2}	1.09	1.09	1.09
Model 3.....	0.80×10^{-2}	0.60×10^{-2}	0.50×10^{-2}	4.11	4.07	3.65

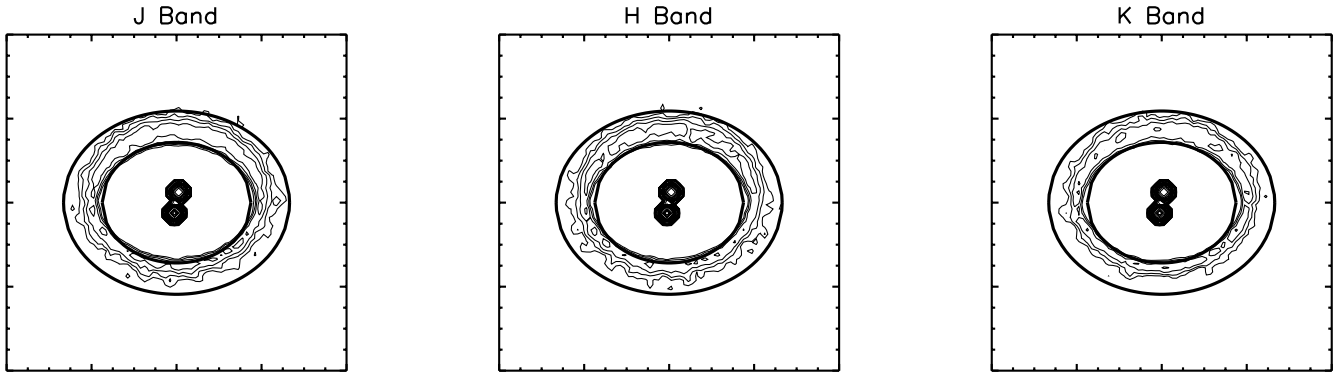

FIG. 2.—Scattered-light simulations at J, H, and K viewed at an inclination of $i = 35°$ for Model 2. Each figure is 800 AU on a side. The lowest contour in each image is at 5×10^{-5} times the peak flux in each image and the contour spacing is at half-magnitude intervals.

model 1 show that the far side of the disk is brighter than the near side.

In order to offset these discrepancies, we explored other values for the scale height, h_0, and inner disk radius. Figure 2 shows model images for $h_0 = 7$ AU and an inner radius of 200 AU, so the scale height at the inner edge of the circumbinary disk is $h(200\ \mathrm{AU}) = 16.6$ AU. This combination of h_0 and inner radius gives the best match of scattered light to the concentric ellipses. However, although the near side is slightly brighter than the far side (Table 3), the NF_λ ratios are smaller than observed by Roddier et al. (1996). Also, the R_λ flux ratios derived for this model are too large. In an attempt to reduce the R_λ flux ratios in our simulations, we reduced the mass of the circumbinary disk. A smaller disk mass results in less scattering and therefore smaller flux ratios. However, we find that the circumbinary disk remains optically thick to scattering over a wide range of disk masses (Table 4). It is not until the circumbinary mass is of order $10^{-4}\ M_\odot$ that the model flux ratios approach those observed. Such a small circumbinary mass is inconsistent with the $0.13\ M_\odot$ derived from millimeter observations. Lowering the dust albedo could help in lowering the flux ratios, but observations indicate that if anything, the dust albedo may be larger than the values we are adopting (e.g., Sellgren, Werner, & Dinnerstein 1992; Whitney et al. 1997; Gordon, Calzetti, & Witt 1997). Since we are choosing to keep the dust parameters fixed for our simulations, we must therefore explore other means of reducing the model flux ratios. In the following section we investigate the effect of small circumstellar disks (as proposed by Roddier et al.) and the extinction that they will introduce prior to light reaching the circumbinary disk.

3.2. *Binary Stars Plus Circumstellar Disks*

Assuming each star has its own small circumstellar disk, described by equation 1, we may use our Monte Carlo technique to calculate the emergent flux from this star plus disk system as a function of viewing angle (see Whitney & Hartmann 1992). The results of such a J band calculation are shown in Figure 3 for a $10^{-4}\ M_\odot$ disk of radius 10 AU, $\beta = \frac{9}{8}$, and a scale height at the stellar surface of $h = 0.03\ R_\star$ (see also Whitney & Hartmann 1992). We may simulate the effects of these small circumstellar disks in our binary star simulation, by releasing photons from the point-like binary stars, but with an angular distribution given by Figure 3, rather than the isotropic photon release adopted in the previous section. Although we are still assuming that the radiation originates from point sources, its angular dependence reproduces that from a star plus disk system. As in our previous models the relative number of photons released from each system is given by the luminosity ratios of Roddier et al. (1996). We further assume that the circumstellar disks are coplanar with the circumbinary disk, resulting in a large reduction in the amount of stellar radiation that can impact the circumbinary disk.

Figure 4 shows scattered-light images for Model 3 in which the circumbinary disk of Figure 2 is illuminated by

TABLE 4

FLUX RATIOS FOR NAKED STARS

Disk Mass ($M_\odot$)	R_J	R_H	R_K
Observed	0.43×10^{-2}	0.78×10^{-2}	0.57×10^{-2}
0.13	3.09×10^{-2}	2.78×10^{-2}	2.27×10^{-2}
10^{-2}	2.70×10^{-2}	2.60×10^{-2}	2.10×10^{-2}
10^{-3}	1.70×10^{-2}	1.20×10^{-2}	0.90×10^{-2}
10^{-4}	0.24×10^{-2}	0.13×10^{-2}	0.08×10^{-2}
10^{-5}	0.23×10^{-2}	0.15×10^{-2}	0.06×10^{-2}

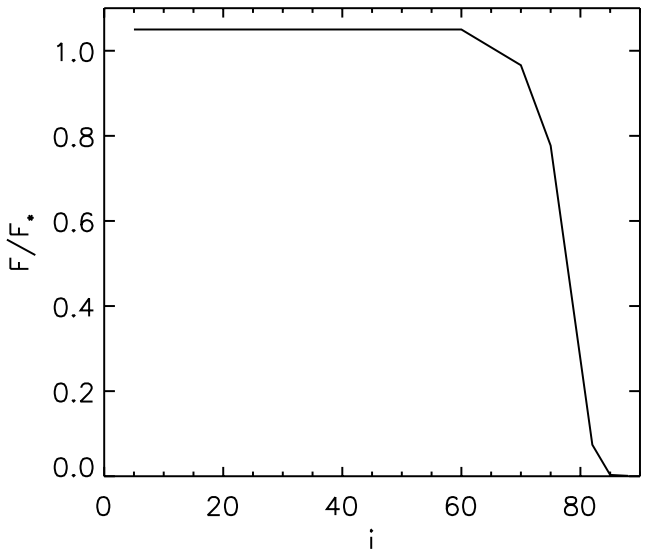

FIG. 3.—Emergent flux as a function of viewing angle for a star surrounded by a $10^{-4}\ M_\odot$ disk of radius 10 AU, $\beta = \frac{9}{8}$, and a scale height at the stellar surface of $h = 0.03\ R_\star$. The flux is larger than the stellar flux at low inclinations due to light scattered from the disk. This angular variation of the emergent flux is used for illuminating the circumbinary disk models presented in Fig. 4.

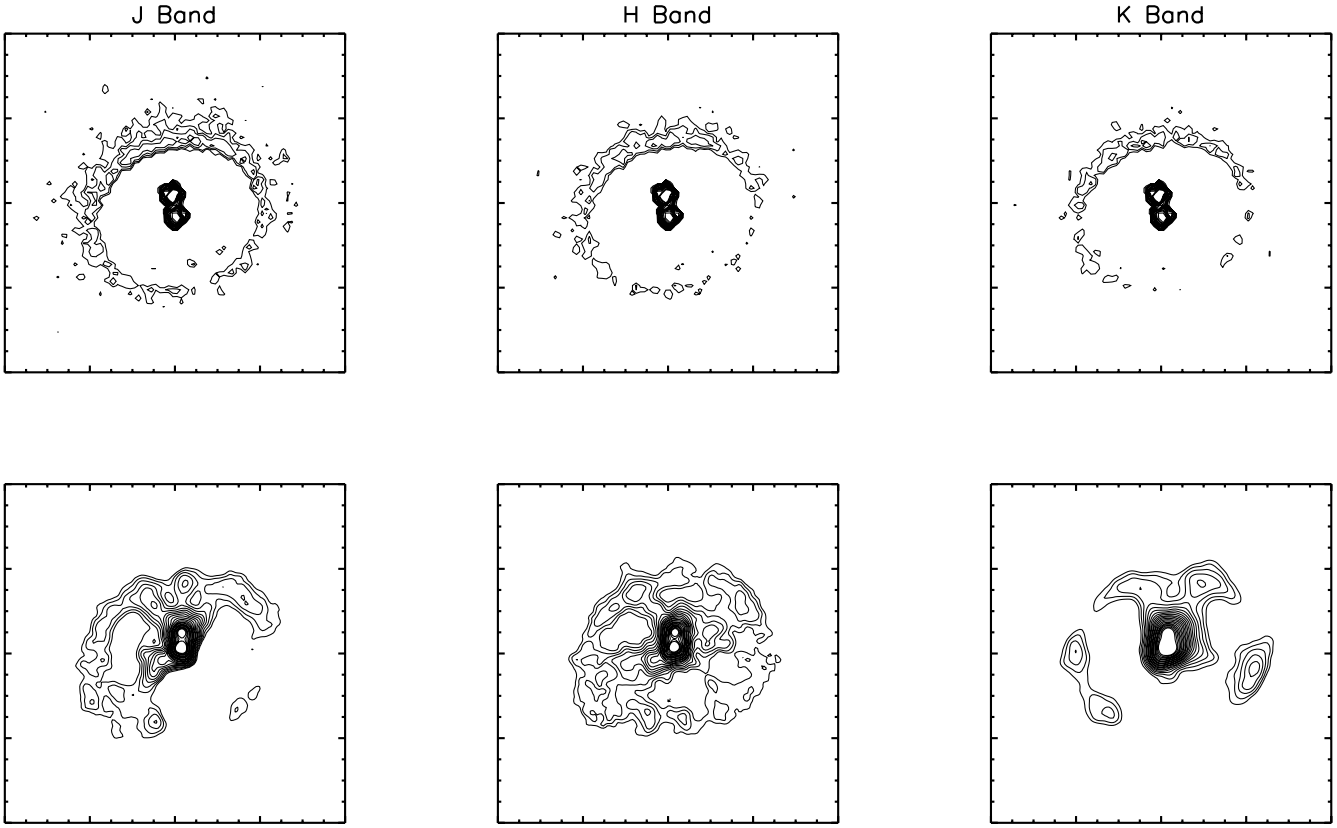

FIG. 4.—Upper three panels show the scattered-light simulations for model 3 at J, H, and K viewed at an inclination of $i = 35°$. The models have been rotated clockwise by 160° to line up with the near-IR images of Roddier et al. (1966) that are presented in the lower three panels. For the data and models, each figure is 800 AU on a side. The lowest contour in each image is at 2.5×10^{-5} times the peak flux in each image and the contour spacing is at half-magnitude intervals.

the star-plus-disk systems of Figure 3. Also displayed, on the same scale and with the same relative contour levels, are the near-IR images obtained by Roddier et al. (1996). Our model images have been rotated clockwise by 160° from those presented in Figures 1 and 2, so that the near (brighter) side of the circumbinary disk is aligned with the near side of the disk inferred from the observations (Roddier et al. 1996; Close et al. 1998). The R_λ flux ratios from this model are consistent with those observed (Table 3). The NF_λ ratios are larger than in Figure 2, showing that the near side of the disk is much brighter for this model. Our simulations match the observed NF_J, but are too large at H and K. We have assumed that the illumination of the circumbinary disk is by stars surrounded by smooth, axisymmetric disks that are coplanar with the circumbinary disk. Clearly any departure from this idealized situation (such as lumpy or noncoplanar disks) could allow more or less light to scatter in the circumbinary disk and could easily change the R_λ and NF_λ ratios from those predicted by our models. In these images in Figure 3, notice the dark lane present on the inner edge of the circumbinary disk. This arises from the large equatorial extinction in the circumstellar disks, producing the observed "shadow" in these model images so that the binary system does not appear to be at the center of the circumbinary disk. Such an asymmetry is seen in the Roddier et al. images and the circumstellar extinction may explain this asymmetry.

Our main conclusions are that small circumstellar disks can provide the required extinction and shadowing effects to reproduce the observed R_λ ratios, and that geometry and illumination effects can also yield NF_λ ratios in line with those observed. Small circumstellar disks are believed to exist around the individual stars because of their signature of IR excess observed in the individual spectra of the binary stars (see Fig. 6 in Roddier et al. 1996). So our modeling has quantitatively confirmed the notion proposed by Roddier et al. that circumstellar extinction plays a crucial role in the formation of the near IR images of the circumbinary disk. The masses that we have adopted for the circumstellar disks should not be taken as accurate determinations. We have assumed that the disks are coplanar and axisymmetric. Deviations from such an ideal configuration (such as noncoplanar or lumpy disks) would allow more starlight to impact the circumbinary disk, increasing the flux ratios and changing the near/far ratios. This could be compensated for by increasing the circumstellar mass and how much the circumstellar disk flares, so as to produce the required circumstellar extinction. With these caveats in mind, our adopted circumstellar disks have masses that are reasonable for disks in a binary system (e.g., Stapelfeldt et al. 1998).

4. ^{13}CO ($J = 1 \rightarrow 0$) LINE PROFILES

In the models presented above we calculated near-IR scattered-light images to compare with the data presented by Roddier et al. (1996). Using the geometry that best reproduced the scattered-light images, we now calculate ^{13}CO ($J = 1 \rightarrow 0$) line profiles and position-velocity maps to compare with the data presented by Dutrey et al. (1994). As with Dutrey et al., we adopt a radial temperature structure $T(r) = T_0(r/100\ \mathrm{AU})^{-q}$. Dutrey et al. adopted $T_0 = 30$ K

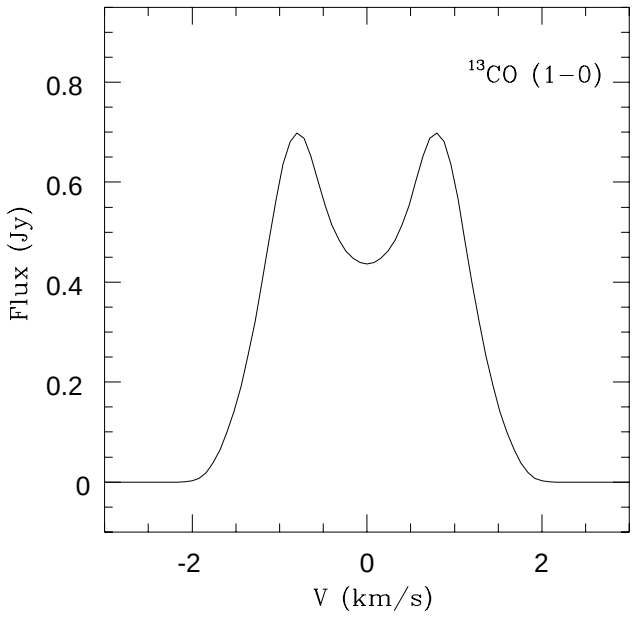

FIG. 5*a*

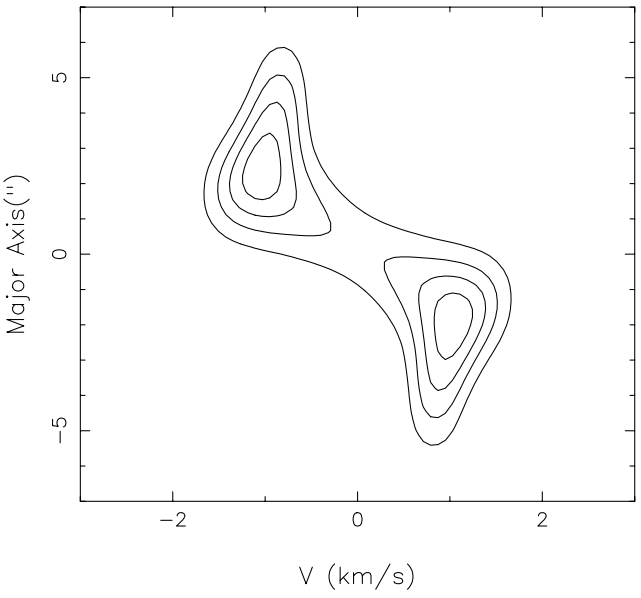

FIG. 5*b*

FIG. 5.—(*a*) ^{13}CO line profiles and (*b*) position-velocity maps for the density structure used to reproduce the scattered-light images. The models have been convolved with a Gaussian beam of FWHM = 2″, and the contour spacing is 1 K (50 mJy/beam).

and $q = 0.5$. However, our scattered-light models show that the illumination of the circumbinary disk is not by isotropic point sources, and this will result in less direct stellar heating, a lower T_0, and a steeper temperature structure. We adopt $T_0 = 20$ K and $q = 0.7$, and set a minimum disk temperature of 3 K, since we find that these values give a good reproduction of the line intensity. The T_0 we adopt is in between that adopted by Dutrey et al. and the $T_0 = 11.4$ K derived by Beckwith et al. (1990). The disk is assumed to be in Keplerian rotation, and we find that the line profile is best reproduced with a velocity $V(r) = 4.0(r/100\ \mathrm{AU})^{-0.5}$ km s^{-1} and a turbulent velocity of 0.2 km s^{-1}. The Keplerian velocity is slightly higher than the 3.3 km s^{-1} of Dutrey et al.

Figure 5*a* shows the model integrated flux density for ^{13}CO ($J = 1 \rightarrow 0$) emission. We achieve good agreement between the observed line profile (Dutrey et al. (1996), Fig. 6) and model results using an abundance of $^{13}\mathrm{CO/H_2} = 2 \times 10^{-8}$, comparable to the abundance derived by Dutrey et al. This supports the finding by Dutrey et al. that CO is underabundant in the GG Tau disk and suggests condensation of CO onto grain surfaces. Our radiation transfer results show that the surface of the flared disk is superthermal. This effect is insignificant in our case because the ^{13}CO line is optically thin in most of the disk. The optical depth, along a line of sight through the disk, becomes 1 in the inner part of the disk ($< 10^{15}$ cm), where the density is higher, is around 0.6 in the center of the disk (10^{15} cm), and becomes 1 again at the outer part of the disk, where the path along the line of sight is larger.

Our position-velocity diagrams (Fig. 5*b*) show slightly more extended emission than the data presented by Dutrey et al. (1994; their Fig. 6). To obtain a better match between models and observations, Dutrey et al. constructed a model disk that had an inner dense ring containing 90% of the mass. This model gives a very large IR optical depth in the ring and is not compatible with the near-IR scattered-light models. Since the CO line emission and mm continuum maps are sensitive to both density and temperature, better agreement between our CO model and the data is obtained with a cooler, steeper temperature law. This point was also made by Dutrey et al., but rejected, as they felt the temperatures required would be too low. However, recent radiation transfer models (Menshchikov & Henning 1997; Chiang & Goldreich 1997; D'Alessio et al. 1998) have shown that the interior of dense disks are much cooler than their surfaces, and with the apparent nonisotropic illumination from the central star plus disk systems in GG Tau, the temperature could be lower than that assumed by Dutrey et al. Until detailed calculations of the temperature structure for such a system are conducted, we cannot discriminate between our smooth, anisotropically illuminated disk model with a cooler temperature that fits the near-IR scattered light and ^{13}CO ($J = 1 \rightarrow 0$) profiles, or the massive ring adopted by Dutrey et al. to fit the CO line and mm continuum data.

5. SUMMARY

We have used detailed Monte Carlo radiation transfer techniques to simulate near IR images and ^{13}CO ($J = 1 \rightarrow 0$) line profile and position-velocity maps to compare with observations of GG Tau's circumbinary disk. The morphology of the near IR observations of Roddier et al. (1996) are best reproduced with a flared circumbinary disk viewed at $i = 35°$, with inner radius 200 AU, a scale height at 100 AU of $h_0 = 7$ AU, and a flaring parameter $\beta = \frac{5}{4}$. However, recent BIMA observations suggest the presence of dust within the GG Tau circumbinary ring (L. Mundy 1998, private communication). This dust may give rise to some of the structures internal to the main dust ring observed by Roddier et al. (1996). Our disk is assumed to have a radial density that decreases as $1/r^2$ and is truncated at a radius of 800 AU, as suggested by millimeter observations (Dutrey et al.). Assuming the disk mass is 0.13 $M_\odot$, we find $\rho_0 = 10^{-14}$ g cm^3 (corresponding to a number density $n_0 = 3 \times 10^9$ cm^{-3}). We note that due to the degen-

eracies in α, h_0, and β (Wood et al. 1998; Burrows et al. 1996) similar morphologies could be obtained with other values for the radial density, scale height, and flaring. In order to obtain scattered flux levels consistent with observations we require the presence of absorbing material in the disk midplane between the stars and the circumbinary disk. We have modeled this with small circumstellar disks (of radius 10 AU and mass 10^{-4} $M_{\odot}$) coplanar with the circumbinary disk. Although this yields scattered-light levels that are close to those observed, the ratio of light scattered from the near and far sides of the disk is larger than observed. We suggest that nonaxisymmetric or "lumpy" disks, as proposed by Roddier et al., could aid in resolving this discrepancy and yield more scattered light from the far side or less from the near side to bring the near/far ratios closer to those observed. Although Close et al. (1998) obtained a good match to the near/far ratios in GG Tau by changing the size distribution and hence scattering phase function of the circumbinary dust, their model consisted of single scattering of starlight off the surface of a flat disk. In our Monte Carlo simulations, we find that the nonplanar circumbinary geometry and the nonisotropic illumination are the most important model components that effect the morphology of the scattered-light images. Multiple scattering is less important with the average number of scatterings (of Monte Carlo "photons" scattered in the circumbinary disk) being 1.25 at J, 1.20 at H, and 1.15 at K.

The ^{13}CO ($J = 1 \rightarrow 0$) line emission and position-velocity maps were modeled with the same density used for the scattered-light images. With this model, we obtained slightly too much emission at large radii. We further suggest a cooler disk with a steeper temperature structure than that used by Dutrey et al. (1994). Such a temperature structure may exist in the inner dense regions of the disk that are hidden from illumination by the binary stars. Also, the shadowing effect of the circumstellar disks required to match the near-IR images will result in less illumination of the circumbinary disk and a lower temperature. Therefore, we cannot as yet discriminate between our model and the dense ring proposed by Dutrey et al. We find an abundance of $^{13}CO/H_2 = 2 \times 10^{-8}$ is required to match the models. This supports the notion of Dutrey et al. of depletion of CO onto grains in a very cold dense circumbinary disk.

We thank C. Roddier for providing us with the near-IR adaptive optics images of GG Tau. Alex Rae conducted a preliminary investigation into the formation of circumbinary scattered-light images. We also thank Barbara Whitney, Jon Bjorkman, Scott Kenyon, David Wilner, and Ted Bergin for helpful comments and discussions. K. W. acknowledges support from NASA's Long Term Space Astrophysics Research Program (NAG5-6039).

REFERENCES

Adams, F. C., Lada, C. J., & Shu, F. H. 1987, ApJ, 312, 788
Adams, F. C., & Shu, F. H. 1986, ApJ, 308, 836
Artymowicz, P., & Lubow, S. H. 1994, ApJ, 421, 651
———. 1996, ApJ, 467, L77
Beckwith, S. V. W., & Sargent, A. I. 1993, ApJ, 402, 280
Beckwith, S. V. W., Sargent, A. I., Chini, R. S., & Gusten, R. 1990, AJ, 99, 924
Bernes, C. 1979, A&A, 73, 67
Burrows, C. J., et al. 1996, ApJ, 473, 437
Chiang, E. I., & Goldreich, P. 1997, ApJ, 490, 368
Clarke, C. J. 1995, in Evolutionary Processes in Binary Stars, ed. R. A. M. J. Wijers, M. B. Davies, & C. A. Tout (Dordrecht: Kluwer), 477
Close, L. M., et al. 1998, ApJ, 499, 883
Crosas, M., & Menten, K. M. 1997, ApJ, 483, 913
D'Alessio, P., Canto, J., Calvet, N., & Lizano, S. 1998, ApJ, 500, 411
Dutrey, A., Guilloteau, S., & Simon, M. 1994, A&A, 286, 149
Fischer, O. Henning, T., & Yorke, H. W. 1994, A&A, 284, 187
Ghez, A. M., White, R. J., & Simon, M. 1997, ApJ, 490, 353
Gordon, K. D., Calzetti, D., & Witt, A. N. 1997, ApJ, 487, 625
Henyey, L. G., & Greenstein, J. L. 1941, ApJ, 93, 70
Kenyon, S. J., & Hartmann, L. 1987, ApJ, 323, 714
Kim, S. H., Martin, P. G., & Hendry, P. D. 1994, ApJ, 422, 164
Koerner, D. W., & Sargent, A. I. 1995, AJ, 109, 2138
Koerner, D. W., Sargent, A. I., & Beckwith, S. V. W. 1993a, Icarus, 106, 2
———. 1993b, ApJ, 408, L93
Lin, D. N. C., & Papaloizou, J. C. B. 1983, in Protostars and Planets III, ed. E. H. Levy & J. I. Lunine (Tucson: Univ. Arizona Press), 749
Menshchikov, A. B., & Henning, T. 1997, A&A 318, 879
Pringle, J. E. 1991, MNRAS, 248, 754
Roddier, C., Roddier, F., Northcott, M. J., Graves, J. E., & Jim, K. 1996, ApJ, 463, 326
Sellgren, K., Werner, M. W., & Dinnerstein, H. L. 1992, ApJ, 400, 238
Shakura, N. I., & Sunyaev, R. A. 1973, A&A, 24, 337
Shu, F. H., Adams, F. C., & Lizano, S. 1987, ARA&A, 25, 23
Simon, M., & Guilloteau, S. 1992, ApJ, 397, L47
Stapelfeldt, K. R., et al. 1998, ApJ, 502, L65
Whitney, B. A., & Hartmann, L. 1992, ApJ, 395, 529
Whitney, B. A., Kenyon, S. J., & Gomez, M. 1997, ApJ, 485, 703
Wood, K., Kenyon, S. J., Whitney, B., & Turnbull, M. 1998, ApJ, 497, 404